Predicting Perfect Adaptation Motifs in Reaction Kinetic Networks

Tormod Drengstig

Department of Electrical Engineering and Computer Science, University of Stavanger, Stavanger, Norway

Hiroki R. Ueda

Center for Developmental Biology, RIKEN, Kobe, Japan

Peter Ruoff*

Centre for Organelle Research, Faculty of Science and Technology, University of Stavanger, N-4036 Stavanger, Norway

Received: July 31, 2008; Revised Manuscript Received: October 02, 2008

Adaptation and compensation mechanisms are important to keep organisms fit in a changing environment. "Perfect adaptation" describes an organism's response to an external stepwise perturbation by resetting some of its variables precisely to their original preperturbation values. Examples of perfect adaptation are found in bacterial chemotaxis, photoreceptor responses, or MAP kinase activities. Two concepts have evolved for how perfect adaptation may be understood. In one approach, so-called "robust perfect adaptation", the adaptation is a network property (due to integral feedback control), which is independent of rate constant values. In the other approach, which we have termed "nonrobust perfect adaptation", a fine-tuning of rate constant values is needed to show perfect adaptation. Although integral feedback describes robust perfect adaptation in general terms, it does not directly show where in a network perfect adaptation may be observed. Using control theoretic methods, we are able to predict robust perfect adaptation sites within reaction kinetic networks and show that a prerequisite for robust perfect adaptation is that the network is open and irreversible. We applied the method on various reaction schemes and found that new (robust) perfect adaptation motifs emerge when considering suggested models of bacterial and eukaryotic chemotaxis.

Introduction

In order to cope with a changing environment, organisms have the ability to adapt[1,2] to persistent external perturbations. Several modes of adaptation exist,[3,4] ranging from no adaptation at all to partial adaptation, perfect adaptation, or overadaptation (Figure 1a). The term perfect adaptation describes a system's response when certain variables return to precisely their original preperturbation values during a stepwise perturbation.

Perfect adaptation has been found in a variety of instances, for example, in bacterial[5−11] and eukaryotic[12] chemotaxis, in certain photoreceptor responses,[13,14] and in MAP-kinase regulation.[15−17] Two concepts have evolved for how perfect adaptation may be understood. In one approach, a fine-tuning/balancing of the rate constants is needed to show perfect adaptation,[8,18−21] while in the other approach, the adaptation process is a network property which needs no fine-tuning.[12,16,22−24] Yi et al.[23] coined the term for this behavior as "robust perfect adaptation" and indicated that this form of adaptation can be formulated in terms of integral feedback,[16,23] a concept employed in control theory.[25−29] Although integral feedback can describe robust perfect adaptation in general terms, it does not directly predict where in a network it will occur.

We became interested in the question of how to predict the location of robust perfect adaptation sites in reaction kinetic networks. By transforming an earlier global approach for the condition of temperature compensation[30,31] to a single reaction site within a network receiving a signal from a receptor, it became evident that a necessary (but not sufficient) condition for robust perfect adaptation is related to the presence of a zero control (sensitivity) coefficient[32−35] of the actual steady-state concentration with respect to the rate constant at this site.[36]

In this paper, we combine kinetic and control engineering methods to predict where in a kinetic network perfect adaptation motifs can occur and how the adaptation kinetics, either robust or nonrobust, can be characterized by their transfer functions and frequency responses.

Computational Methods

MATLAB (www.mathworks.com) was used to determine transfer functions as well as step and frequency responses on linearized models. For comparison with the actual nonlinear model, rate equations were solved numerically by using the FORTRAN subroutine LSODE (Livermore Solver of Ordinary Differential Equations)[37] and SIMULINK (www.mathworks.com).

Results

Transfer Function and Adaptation Kinetics. We consider a reaction kinetic network with M chemical components (I_j) and N elementary reactions steps, where each step i is associated with a rate constant k_i. The network can be stimulated by changing one of the rate constants (k_i) by means of a step

* To whom correspondence should be addressed. Tel.: (47) 5183-1887. Fax: (47) 5183-1750.

10.1021/jp806818c CCC: $40.75

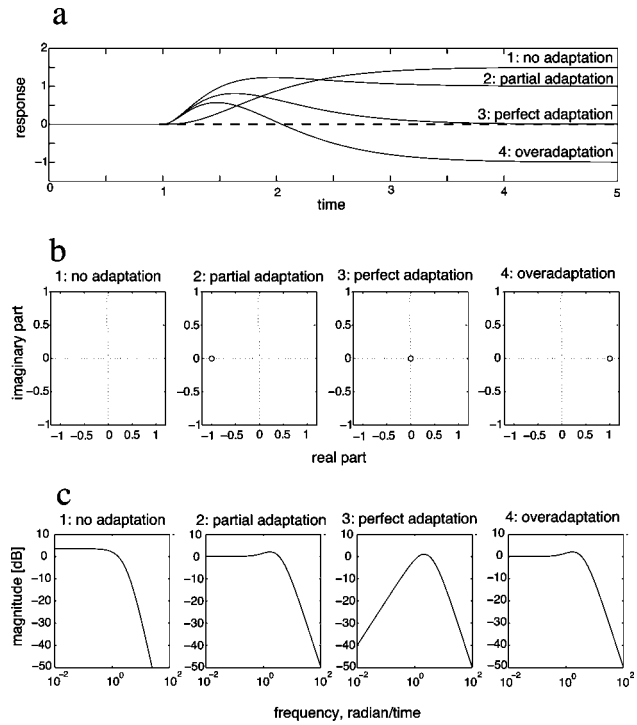

Figure 1. (a) Step responses, (b) zeros, and (c) frequency responses for four different transfer functions showing (1) no adaptation, (2) partial adaptation, (3) perfect adaptation, and (4) overadaptation. The four transfer functions are described by $H_i(s) = n_i(s)/d(s)$, $i = 1,..., 4$, with the same denominator $d(s) = (0.2s + 1)(0.35s + 1)(0.45s + 1)$, that is, a third-order overdamped system. In order to visualize the impact of different zeros, the numerators are $n_1(s) = 1.5$, $n_2(s) = (s + 1)$, $n_3(s) = s$, and $n_4(s) = s - 1$.

function. This stimulation is considered to occur due to a signal from a receptor acting specifically and proportionally (at least at low stimulation amplitudes) on k_i due to an external stepwise perturbation of the receptor. In this respect, the rate constants are considered to be dependent upon time t. The kinetics of the network are described by the rate equations for each chemical component I_j

$$\frac{dI_j(t)}{dt} = f_j(k_1(t), ..., k_N(t), I_1(t), ..., I_M(t)) \tag{1}$$

In order to find the steady-state concentrations $I_{j,ss}$, the derivatives in eq 1 are set to zero, and the resulting equations are solved with respect to the steady-state concentrations.

Perfect adaptation sites in a network are identified by applying a stepwise perturbation on each rate constant k_i and finding the corresponding perfectly adapted responses for some of the intermediates I_j. A necessary (but not sufficient) condition for robust perfect adaptation is that the control coefficient[32,38] $C^{I_{j,ss}}_{k_i} = \partial \ln I_{j,ss}/\partial \ln k_i$ becomes zero. This condition indicates that the steady-state concentration $I_{j,ss}$ is independent of (changes in) k_i. $C^{I_{j,ss}}_{k_i} = 0$ is only a necessary condition because there may be steady-state concentrations which are completely independent of certain rate constants. For example, the change of a rate constant in an irreversible chain of consecutive reactions will not affect any steady-state level located upstream in the chain. We call such a relationship between rate constants k_i and steady-state levels $I_{j,ss}$ disconnected. Therefore, an additional functional relationship is needed, which describes if and how the steady-state concentration $I_{j,ss}$ and rate constant k_i are connected to each other. Such a description is given by the transfer function matrix $H(s)$.[25−27,29] In order to find $H(s)$, eq 1 is first linearized around the steady-state (ss) values $\mathbf{I_{ss}} = [I_{1,ss},..., I_{M,ss}]$ and the preperturbation values of $\mathbf{k} = [k_1,..., k_N]$, giving the following linear model

$$\Delta\dot{\mathbf{I}}(t) = A\cdot\Delta\mathbf{I}(t) + B\cdot\Delta\mathbf{k}(t) \tag{2}$$

where $\Delta\mathbf{k}(t) = [\Delta k_1(t),..., \Delta k_N(t)]^T$ is a vector of small deviations around the preperturbation values of $\mathbf{k}$, and $\Delta\mathbf{I}(t) = [\Delta I_1(t),..., \Delta I_M(t)]^T$ is a vector of small deviations around the steady-state concentrations $\mathbf{I_{ss}}$. The matrix A is the system matrix ($M \times M$) defined by $A_{ij} = (\partial f_i/\partial I_j)|_{ss}$, and B is the input matrix ($M \times N$) defined by $B_{ij} = (\partial f_i/\partial k_j)|_{ss}$. Applying the Laplace transform (from the real-valued t axis to the complex-valued s plane) to the linearized model in eq 2 gives the $M \times N$ transfer function matrix $H(s)$ as[25]

$$H(s) = \frac{\Delta\mathbf{I}(s)}{\Delta\mathbf{k}(s)} = (sI - A)^{-1}B \tag{3}$$

$H(s)$ describes the connections between a small change in all possible inputs, here the array of Laplace transformed rate constants $\Delta\mathbf{k}(s) = [\Delta k_1(s),..., \Delta k_N(s)]^T$, and the resulting small changes in all possible outputs, that is, the array of all Laplace transformed concentration changes $\Delta\mathbf{I}(s) = [\Delta I_1(s),..., \Delta I_M(s)]^T$. I is the identity matrix ($M \times M$). The matrix $(sI - A)^{-1}$ is calculated by means of the cofactors of $(sI - A)$ divided by the determinant of $(sI - A)$. The condition $\det(sI - A) = 0$ determines the poles of the system, which are identical to the eigenvalues of $(sI - A)$. In general, the elements $H_{ji}(s)$ of the transfer function matrix $H(s)$ are written as

$$H_{ji}(s) = \frac{\Delta I_j(s)}{\Delta k_i(s)} = \frac{K\cdot\prod_{r=1}^{n}(s - z_r)}{\prod_{q=1}^{m}(s - p_q)} = \frac{n(s)}{d(s)} \tag{4}$$

where z_r are the transfer function's zeros, p_q are the poles, and K is the gain. As indicated in eq 4, $H_{ji}(s)$ is described as the ratio between two polynomials, the numerator polynomial $n(s)$ and the denominator polynomial $d(s)$.

Robust and Nonrobust Perfect Adaptation. When for a given $H_{ji}(s)$ $n(s)$ has a zero in origo of the s plane regardless of the values in any of the rate constants, the system shows robust perfect adaptation in $I_j(t)$ with respect to a stepwise increase in the rate constant k_i (Figure 1a). The reason for this is that the solution $s = 0$ for $n(s) = 0$, as shown in case 3 in Figure 1b, is rate-constant-independent. Hence, a variation in k_i will not affect the steady-state concentration of $I_j(t)$. In situations when the solution to $n(s) = 0$ has a zero in origo of the s plane but this solution is dependent on the values of certain rate constants, the system shows nonrobust (rate-constant-dependent) perfect adaptation in $I_j(t)$ with respect to a stepwise change in k_i.

Partial Adaptation and Overadaptation. Partial adaptation (Figure 1a) is observed when the solution to $n(s) = 0$ is real and lies in the left half of the s plane (Figure 1b). Overadaptation is observed when the solution to $n(s) = 0$ is real and lies in the right half of the s plane (Figure 1b). In both cases, the solution to $n(s) = 0$ will be rate-constant-dependent.

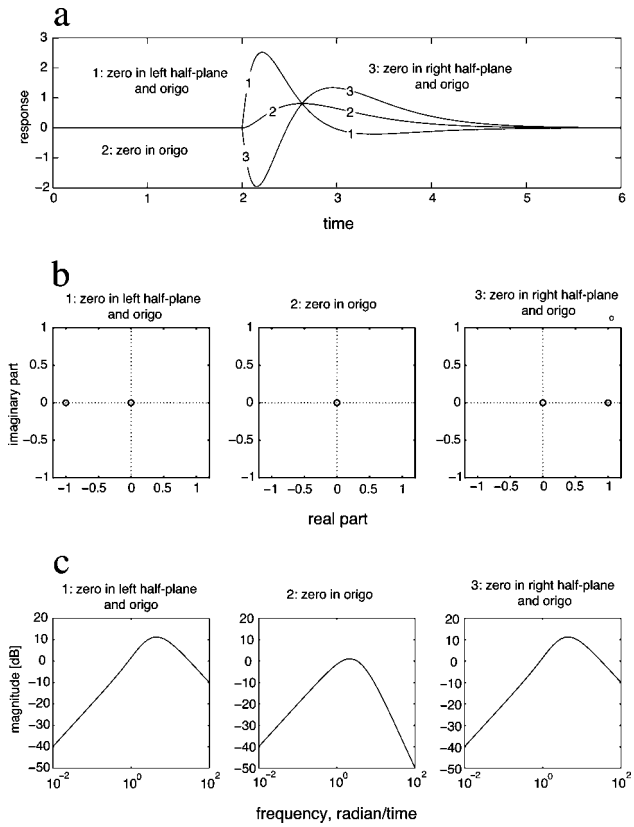

Figure 2. (a) Step responses, (b) zeros, and (c) frequency responses for three different transfer functions, all showing perfect adaptation, that is, they all have at least a zero in origo. All three transfer functions are given as $H_i(s) = n_i(s)/d(s)$, $i = 1,..., 3$, with the same denominator as that in Figure 1. The basic transfer function has only a zero in origo, that is, $n_2(s) = s$. In order to visualize the impact of an additional zero in the left and right half-planes, respectively, the numerators of the two other transfer functions are $n_1(s) = (s + 1)s$ and $n_3(s) = (1 - s)s$.

No Adaptation. If $n(s)$ is a constant and does not have any zeros, no adaptation can be observed (Figures 1a,b).

Figure 1 summarizes the various adaptation types with the respective zeros for $n(s)$ and the corresponding frequency responses shown as Bode plots (Figure 1c, only magnitudes are shown). In the case $H_{ji}(s) = 0$, $I_{j,ss}$ is (what we called) "disconnected" from the rate constant k_i, and consequently, $C^{I_{j,ss}}_{k_i} = 0$.

Influence of the Transfer Function's Poles and Zeros on Adaptation Kinetics. The solution to $d(s) = 0$ identifies the poles of the transfer function. If the poles are negative and real, the system is overdamped, and the step response has no overshooting. If the poles are complex conjugated with a negative real part, the system is underdamped, and the step response shows overshooting. However, the total response of a system will be determined by both the poles and the zeros of the transfer function. Figure 2 shows how the step response of a system with a zero in origo (midfigure) is influenced by an additional zero in the left half-plane (left figure) and by an additional zero in the right half-plane (right figure), leading to different perfect adaptation responses.

In the following, we will illustrate the above conditions for different "perfect adaptation motifs" and show how changes in these motifs can alter the adaptation response.

Conditions for Robust Perfect Adaptation. To get robust perfect adaptation in reaction kinetic networks, two conditions are necessary. The first condition is that the network needs to be open, that is, capable of maintaining a steady state. Closed systems, which are confined by the Principle of Detailed Balance,[44] approach equilibrium and will generally not exhibit, as illustrated below, robust perfect adaptation. However, certain closed systems which contain positive and/or negative feedback loops can transiently exhibit oscillations and steady states[55] and may therefore, during such a transient, show robust perfect adaptation. The second condition to be met in order to get robust perfect adaptation is that the network contains one or more irreversible reaction steps. The placement of these irreversible reactions within the network is crucial for getting robust perfect adaptation (see below).

To illustrate this, we consider the following reversible two-component system of first-order reactions, where the wavy line indicates a (receptor-mediated) stepwise stimulation in k_2

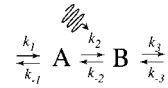

(S1)

The corresponding transfer function $H_{B,k_2}(s)$ is

$$H_{B,k_2}(s) = \frac{\Delta B(s)}{\Delta k_2(s)} = \frac{A_{ss}(s + k_{-1})}{s^2 + (k_3 + k_{-1} + k_{-2} + k_2)s + k_3(k_2 + k_{-1}) + k_{-1}k_{-2}} \quad (5)$$

Since the solution to $n(s) = 0$ for $H_{B,k_2}(s)$ is given by $s = -k_{-1}$, a step in k_2 will show partial adaptation in $B(t)$ as schematically indicated in case 2 of Figure 1b. When $k_{-1} = 0$, $H_{B,k_2}(s)$ has a zero in origo, and a stepwise change in k_2 will now lead to robust perfect adaptation in $B(t)$. A more detailed description of the steady states of this system together with a derivation of eq 5 is given in the Supporting Information.

Thus, a simple motif that can show robust perfect adaptation is scheme M1 where the irreversibility in the first step is essential

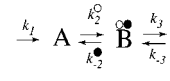

(M1)

for getting robust perfect adaptation in $B(t)$ through a stepwise stimulation of k_2 (or k_{-2}). To get a rapid overview where, in the network, robust perfect adaptation occurs, circular tags are placed at the rate constants (inputs) and at the associated perfectly adapting intermediates (outputs), as indicated in scheme M1.

In the following, we analyze the adaptation response for a variety of irreversible (nonequilibrium) steady-state networks, where some of them are related to adaptation dynamics observed in biological systems.

Network Size and Frequency Response. We consider the following chain of consecutive reactions. Circular tags indicate

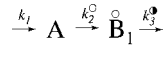

(M2)

the rate constants (inputs) and the associated intermediates (outputs) which show robust perfect adaptation. For example,

robust perfect adaptation is observed in every B_i when k_2 undergoes a stepwise change. The transfer function from the input $\Delta k_2(s)$ to the various ΔB_i's is given by

$$H_{B_l,k_2}(s) = \frac{\Delta B_l(s)}{\Delta k_2(s)} = \begin{cases} \dfrac{A_{ss} \cdot s}{\prod_{j=2}^{l+2}(s + k_j)} & \text{if } l = 1 \\ \dfrac{A_{ss} \cdot s \prod_{i=3}^{l+1} k_i}{\prod_{j=2}^{l+2}(s + k_j)} & \text{if } 2 \le l \le n \end{cases} \quad (6)$$

In both cases of eq 6, the only solution to the numerator polynomial $n(s) = 0$ is $s = 0$, that is, a zero in origo independent of the rate constants.

Besides studying the step response of a system, we can analyze how a system responds to external periodic stimulations.[25,39] This is generally done with a sinusoidal perturbation with a varying frequency ω, which is applied to the linearized model. The amplitudes and phases are determined as a function of ω and presented in form of a Bode plot.[25,27]

Figure 3 shows the step responses and Bode plots for M2 with $n = 6$. Although each of the B_i's shows perfect adaptation (Figure 3a) with similar adaptation kinetics, the frequency responses for the B_i's differ when a sinusoidal perturbation is applied to k_2. With increasing n in scheme M2 the negative slope at high frequencies ω (Figure 3b) will decrease by an additional 20 dB per decade change in ω for each B_i that is added to the network. This means that for a given experimental result where the step response for an intermediate looks like one of the responses in Figure 3a, the size (or the order) of the network cannot be determined unless a frequency response as shown in Figure 3b,c is obtained.

Application of Consecutive Reaction Models. Lumping all intermediates B_i of scheme M2 into a single variable B gives motif M1*, which has also been studied by Hao et al.[16] The

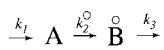

(M1*)

step response of $B(t)$ is shown in Figure 4a, and this response is strikingly similar to the photoadaptation in *Limulus* as

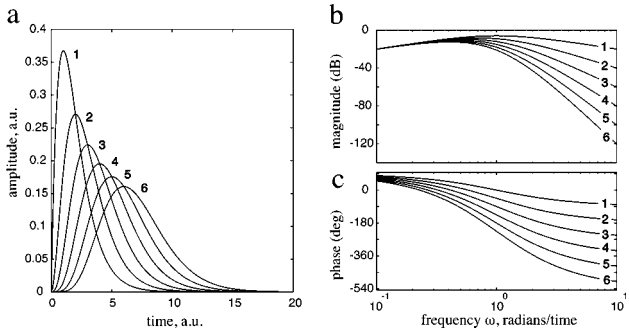

Figure 3. (a) Step responses for the first six B_i's (identified by their i's) in scheme M2 when a step is applied on k_2. Rate equations are $dA/dt = k_1 - k_2 \cdot A$, $dB_1/dt = k_2 \cdot A - k_3 \cdot B_1$, and $dB_i/dt = k_{i+1} \cdot B_i - k_{i+2} \cdot B_i$, where all rate constants are, for the sake of simplicity, set equal to 1.0. Panels (b) and (c) show the corresponding Bode plot, that is, the influence of frequency on the magnitude and phase of the six B_i's, respectively.

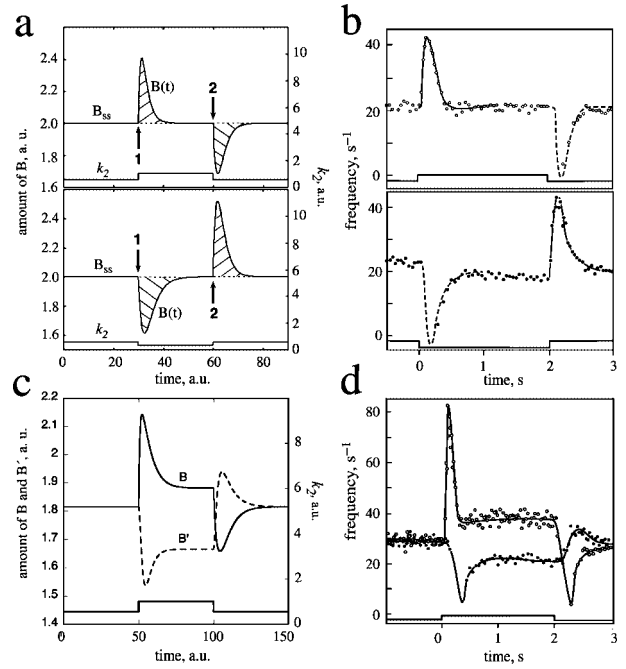

Figure 4. (a, upper panel) Robust perfect adaptation in $B(t)$ of scheme M1* with rate equations $dA/dt = k_1 - k_2 \cdot A$ and $dB/dt = k_2 \cdot A - k_3 \cdot B$. The time and concentrations are given in arbitrary units (a.u.). Rate constant values are $k_1 = 1.0$, $k_2 = 0.55$, and $k_3 = 0.5$. At time $t = 30$, (indicated by **1**), k_2 is increased from 0.55 to 1.0 and then reset to 0.55 at $t = 60$ (at **2**). Hatched areas indicate the amount of released/absorbed B during adaptation. The amount of released/absorbed B during adaptation is given by $(f - 1)k_1/fk_2k_3$, where f describes the stimulation strength, that is, the ratio between the perturbed k_2 (k_2^{per}) and its preperturbed value (k_2) with $k_2^{per} = f \cdot k_2$ (see Supporting Information). This indicates that for high stimulations ($f \gg 1$), the amount of released/absorbed B becomes independent of the stimulation strength f. (a, lower panel) Same system as that in the upper panel, but at $t = 30$ (at **1**), k_2 is decreased from 0.55 to 0.316. At **2** ($t = 60$), k_2 is reset to 0.55. (b) Photoadaptation with respect to a stepwise perturbation of a single photoreceptor in *Limulus*. Shown are changes in the optic nerve discharge frequency for a 2 s incremental flash (upper panel) or a 2 s decremental flash (lower panel). Open and closed circles represent experimental determinations of the nerve's discharge frequencies. The bottom lines in the upper and lower panels indicate the onset and termination of the stimulus. Redrawn after Figure 16 from Ratliff et al.[13] (c) Partial adaptation in B and B' of two coupled M1* motifs (scheme M1**) showing close resemblance to experimental observations (Figure 4d). The following rate equations and rate constants have been used: $dA/dt = k_1/(K_{I_1} + A') - k_2 \cdot A$; $dB/dt = k_2 \cdot A - k_3 \cdot B/(K_{I_2} + A')$; $dA'/dt = k_4/(K_{I_1} + A) - k_5 \cdot A'$; and $dB'/dt = k_5 \cdot A' - k_6 \cdot B'/(K_{I_2} + A)$, with $k_1 = k_4 = 1.0$, $k_2 = k_5 = 0.55$, $k_3 = k_6 = 0.5$, $K_{I_1} = 0.5$, and $K_{I_2} = 0.35$. At $t = 50$, k_2 is increased from 0.55 to 1.0 and reset to 0.55 at $t = 100$. (d) Partial adaptation in two adjacent photoreceptors of *Limulus* (redrawn after Figure 17 from Ratliff et al.[13]). One receptor was constantly illuminated (black dots), while the other receptor (open circles) received an increased illumination between 0 and 2 s and was reset to its preperturbation value after 2 s.

determined by measuring the activity (discharge frequency) of a single optic nerve[13] shown in Figure 4b.

Remarkably, when two robust perfect adaptation motifs M1* are coupled together by mutual inhibition as shown in scheme M1** we observe adaptation responses which are not only

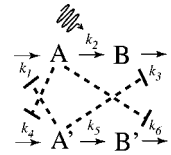

(M1**)

radically different from the isolated motif's (M1*) responses but which show a striking similarity to experimental observations when two photoreceptors of *Limulus* are mutually inhibiting each other[13] (Figure 4c,d)!

This suggests that schemes M1* or M1**, despite their simplicity, could be considered as building blocks for the photoadaptation responses of single and coupled optic nerves in *Limulus*.

Moreover, Brodie et al.[40] studied the frequency response of the *Limulus* lateral eye. Assuming a reaction model as scheme M2, the experimental Bode plot in the Brodie et al. study (Figure 4 in ref 40) indicates a network length of $n \approx 16$ (including models of experimental setup) downstream from the site at which the signal from the receptor is perceived.

Influence of Feedback and Feedforward Loops. Feedback and feedforward loops are common regulatory elements. When including negative feedback or positive feedforward loops in consecutive networks, we generally observe additional over- or undershooting behaviors, but the distribution of the robust perfectly adapted sites within the network remains mostly unaffected. A more detailed description of these behaviors is given in the Supporting Information.

Cyclic Reactions. Turning to cyclic reactions, we found networks that can show both rate-constant-independent (robust) and rate-constant-dependent (nonrobust) perfect adaptation. For the sake of simplicity, we consider here cyclic schemes with three intermediates. A selection of four schemes (**1**−**4**) is given in M3. Although reaction scheme **1** has an irreversible input (k_1), the two output reactions with rate constants k_3 and k_5 produce a transfer function matrix $H(s)$ where none of its elements $H_{ji}(s)$ have a zero in the origo independent of the rate constants.

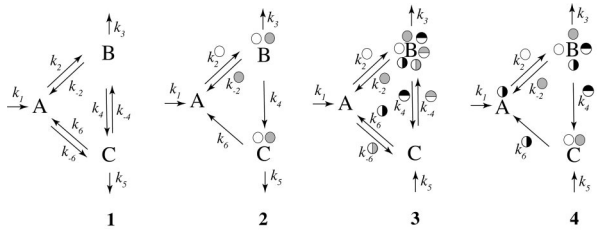

(M3)

Therefore, no robust perfect adaptation can be obtained for this scheme. However, the transfer function from $\Delta k_4(s)$ to $\Delta A(s)$

$$H_{A,k_4}(s) = \frac{n(s)}{d(s)} = \frac{B_{ss}((-k_{-2} + k_6)s - k_5k_{-2} + k_6k_3)}{d(s)} \quad (7)$$

has the following solution to $n(s) = 0$

$$s = \frac{k_5k_{-2} - k_6k_3}{-k_{-2} + k_6} \quad (8)$$

which is rate-constant-dependent. Therefore, a zero in origo for $H_{A,k_4}(s)$ is obtained with perfect adaptation in $A(t)$ when a step perturbation is applied to k_4 if $k_5k_{-2} - k_6k_3 = 0$. Otherwise, partial adaptation or overadaptation (dependent on the values of the rate constants) can be observed. Thus, scheme **1** can demonstrate rate-constant-dependent nonrobust perfect adaptation.

By increasing the number of irreversible steps in **1**, intermediates *B* and *C* become robust perfect adapted (see scheme **2**). No robust perfect adaptation in *A* is observed even when $k_{-2} = 0$. Reversing one of the output reactions in scheme **1** (k_5, see scheme **3**), *B* shows robust perfect adaptation with respect to all rate constants in the ring. Increasing the number of irreversible steps of scheme **3** leads, as shown in **4**, to robust perfect adaptation in all intermediates for stepwise perturbations in different k_i. This illustrates, as already seen for consecutive reaction M1, that the presence of irreversibility and the placement of input and output reactions are crucial for the occurrence of robust perfect adaptation. We found it interesting that in scheme **3** (and in larger cyclic networks) all types of adaptation responses can be observed (Figure 5).

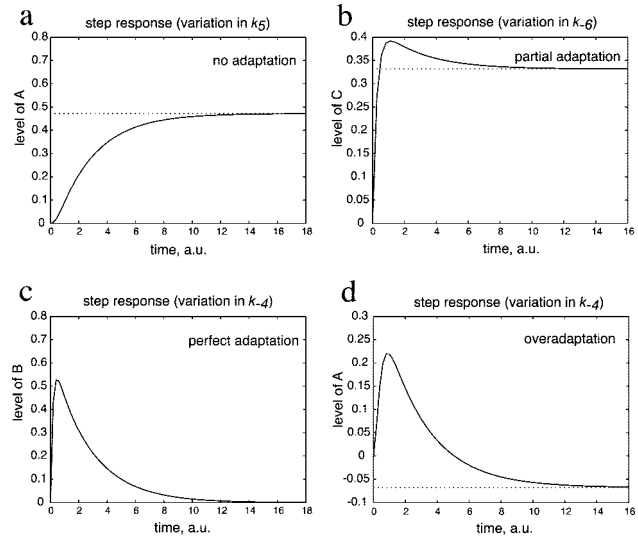

Figure 5. Different adaptation kinetics observed for scheme **3** in M3. (a) No adaptation in *A* for a step perturbation in k_5, (b) partial adaptation in *C* for a step perturbation in k_{-6}, (c) perfect (robust) adaptation in *B* for a step perturbation in k_{-4}, and (d) overadaptation in *A* for a step perturbation in k_{-4}. Rate equations: $dA/dt = k_1 - (k_2 + k_{-6})\cdot A + k_6\cdot C + k_{-2}\cdot B$, $dB/dt = k_2\cdot A - (k_4 + k_{-2} + k_3)\cdot B + k_{-4}\cdot C$, and $dC/dt = k_5 - (k_{-4} + k_6)\cdot C + k_4\cdot B + k_{-6}\cdot A$, with rate constants $k_1 = 1.1$, $k_2 = 1.2$, $k_{-2} = 1.7$, $k_3 = 1.3$, $k_4 = 1.4$, $k_{-4} = 1.8$, $k_5 = 1.5$, $k_6 = 0.1$, and $k_{-6} = 1.9$.

Schemes **2** and **4** of M3 show a close resemblance to the Barkai−Leibler (BL) model[22] of bacterial chemotaxis. The BL model has been discussed[41] using the (thermodynamically) closed form as shown in M4

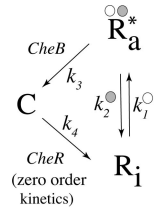

(M4)

The presence of a zero-order reaction step from *C* to R_i assures perfect adaptation in the active form of the receptor R_a^* when applying a stepwise perturbation to k_1 or k_2. In view of the results for schemes **2** and **4** of M3, the presence of a zero-order term in M4 is not absolutely required when describing scheme M4 as an open far-from-equilibrium steady-state system[42,43] by explicitly including system input and system output reactions. It may also be noted that by representing scheme M4, as shown, formally as a closed system,[41] it violates the Principle of Detailed Balance[44] and may, for certain rate constant values, lead to negative concentrations in *C*.

TABLE 1: Overview over $k_j \rightarrow k_i$ Substitutions (scheme *M5*)

index *i*	substituted by index *j*					
2	*1*	**6**	**3**	**6**	**3**	*1*
4	*3*	**1**	**6**	*3*	**1**	**6**
5	*6*	**3**	**1**	**1**	*6*	**3**
number of perfect adaptations	0	3	3	2	2	2

Scheme M5 shows a model suggested by Levchenko and Iglesias[12] in order to describe perfect adaptation in eukaryotic chemotaxis. In this model, an activator *A* drives the receptor to its active form R_a^*, while an inhibitor *I* converts the active receptor into an inactive form R_i.

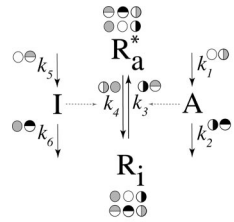

(M5)

Levchenko and Iglesias observed that perfect adaptation is obtained when activation and inhibition of the receptor are mediated by a common signal which activates *A* and *I* by a fixed proportion, that is, $k_5^{\text{per}} = \alpha k_1^{\text{per}}$, where α is any real positive constant. This suggestion for getting perfect adaptation is indicated in scheme M5 by white circular tags at k_5 and k_1 with corresponding white tags at R_a^* and R_i (indicating that both R_a^* and R_i show perfect adaptation). However, by combining the method of zero control coefficients with an analysis of the corresponding transfer functions, five additional possibilities for perfect adaptation can be found, complementing the suggestion by Levchenko and Iglesias. Assuming first-order kinetics,[12] the steady-state concentration of active receptor $R_{a,\text{ss}}^*$ can be expressed in terms of the total receptor concentration $R_{\text{tot}} = R_{a,\text{ss}}^* + R_{i,\text{ss}}$ as (see Supporting Information)

$$R_{a,\text{ss}}^* = \frac{k_1 k_3 k_6}{k_1 k_3 k_6 + k_2 k_4 k_5} R_{\text{tot}} \tag{9}$$

From eq 9, we see that for any substitution $k_i = \alpha k_j$ with $i \in \{2, 4, 5\}$ and $j \in \{1, 3, 6\}$, the control coefficient $C_{k_j}^{R_{a,\text{ss}}^*} = \partial \ln R_{a,\text{ss}}^* / \partial \ln k_j$ becomes zero, suggesting that a common stepwise activation of k_i and k_j ($k_i^{\text{per}} = \alpha k_j^{\text{per}}$) may lead to perfect adaptation. Inspecting the corresponding transfer functions (see Supporting Information), it was found that perfect adaptation is observed in six cases (indicated in scheme M5) out of the nine possibilities that are suggested by a zero control coefficient $C_{k_j}^{R_{a,\text{ss}}^*}$ (data not shown). Table 1 shows all possible rate constant substitution combinations and the resulting number of perfect adaptation possibilities. In Table 1, substitutions which lead to perfect adaptation are indicated in boldface, while those showing no perfect adaptation are indicated in italic.

Discussion

Adaptation processes are important for providing robustness[45,46] to biological systems. To our knowledge, no systematic attempts have so far been made to investigate the possible adaptation responses (Figure 1) in reaction kinetic networks. Here, we have shown how robust perfect adaptation sites and their responses (Figure 2) can be identified by finding zero control coefficients and by analyzing the corresponding transfer functions. Somewhat to our surprise, already small networks can show a relatively large number of robust perfect adaptation sites, which, during evolution, may have been of importance where in a network the signal from a receptor was received. For certain cyclic networks such as scheme **3** of M3, we can even observe simultaneously all adaptation types (Figure 1) in the same network (Figure 5).

A prerequisite to observe robust perfect adaptation is the presence of irreversibility in the network (as seen in the transition from scheme S1 to M1) and treating the network as an open far-from-equilibrium system.[43,42]

While the identification of robust perfect adaptation sites can be linked to the identification of (exact) zero control coefficients and the analysis of the associated transfer functions, the determination of nonrobust (rate-constant-dependent) adaptation sites in a reaction network is less straightforward. It requires an analysis on how control coefficients depend on the rate constants. In addition, rate-constant-dependent adaptation may even occur in the presence of nonzero control coefficients when receptor signals from the same environmental variable are acting at different sites in the network.

To illustrate this latter case (which can be considered as an extension of the $k_i^{\text{per}} = \alpha k_j^{\text{per}}$ suggestion by Levchenko and Iglesias),[12] consider a network where component $I_{j,\text{ss}}$ is dependent on a subset of *P* rate constants. Each rate constant $\{k_i\}_{i=1,\ldots,P}$ is associated with a receptor signal from the same environmental variable Θ (light, a hormone, etc.) changing the values of the k_i's through Θ. The influence of Θ on $I_{j,\text{ss}}$ can be written as

$$\frac{\mathrm{d} \ln I_{j,\text{ss}}}{\mathrm{d} \ln \Theta} = \sum_{i=1}^{P} C_{k_i}^{I_{j,ss}} \frac{\partial \ln k_i}{\partial \ln \Theta} \tag{10}$$

When $C_{k_i}^{I_{j,\text{ss}}} \neq 0$, perfect adaptation may still be possible, but positive and negative contributions of the $C_{k_i}^{I_{j,\text{ss}}}$'s are needed such that eq 10 becomes zero. This type of balancing approach requires a fine-tuning of the parameters $\partial \ln k_i / \partial \ln \Theta$ for a given set of control coefficients. Equation 10 has been suggested as a mechanism for temperature compensation[47,48] of circadian rhythms[30,47,49−52] and steady-state fluxes[31] in ectotherms. An analysis of the influence of temperature on reaction kinetic networks in terms of control coefficients and transfer functions will be given elsewhere.

The analysis presented here is based on linearizing a system around a steady state. This has the advantage of making the analysis more tractable.[26] Although a linearized model is a good approximation for a nonlinear system when applying small perturbations,[27,29,53,54] the linearized system may not describe correctly system responses when using large perturbations. In this respect, studies using linearized models may be complemented by numerical techniques[54,56,57] or by trying to apply methods such as feedback control.[29]

Adaptation mechanisms contribute to the robustness of biological systems, and there are attempts to provide a mathematical description of robustness.[45,46] In this respect, we think that the here-described methods are useful in identifying and characterizing adaptation responses within reaction kinetic networks.

Acknowledgment. We thank Morten Tengesdal and Ludger Rensing for comments on the manuscript. This research was supported, in part, by the National Science Foundation under Grant No. PHY05-51164. The KITP preprint number of this manuscript is NSF-KITP-07-213.

Supporting Information Available: Derivations of the transfer functions for scheme S1 and scheme M5, derivation of the amount of released/absorbed *B* during adaptation in scheme M1*, and a description of the influences of negative feedback and positive feedforward loops on adaptation behaviors in consecutive reactions. This material is available free of charge via the Internet at http://pubs.acs.org.

References and Notes

(1) Hochachka, P. W.; Somero, G. N. *Biochemical Adaptation. Mechanism and Process in Physiological Evolution*; Oxford University Press: Oxford, U.K., 2002.

(2) Holland, J. H. *Adaptation in Natural and Artificial Systems*; MIT Press: Cambridge, MA, 1992.

(3) Asthagiri, A. R.; Lauffenburger, D. A. *Annu. Rev. Biomed. Eng.* **2000**, *2*, 31–53.

(4) Koshland, D. E., Jr.; Goldbeter, A.; Stock, J. B. *Science* **1982**, *217* (4556), 220–5.

(5) Berg, H. C.; Tedesco, P. M. *Proc. Natl. Acad. Sci. U.S.A.* **1975**, *72* (8), 3235–9.

(6) Alon, U.; Surette, M. G.; Barkai, N.; Leibler, S. *Nature* **1999**, *397* (6715), 168–71.

(7) Bray, D. *Proc. Natl. Acad. Sci. U.S.A.* **2002**, *99* (1), 7–9.

(8) Mello, B. A.; Tu, Y. *Biophys. J.* **2003**, *84* (5), 2943–56.

(9) Berg, H. C. *E. coli in Motion*; Springer-Verlag: New York, 2004.

(10) Mello, B. A.; Tu, Y. *Biophys. J.* **2007**, *92* (7), 2329–37.

(11) Hansen, C. H.; Endres, R. G.; Wingreen, N. S. *PLoS Comput. Biol.* **2008**, *4*, 0014−0027.

(12) Levchenko, A.; Iglesias, P. A. *Biophys. J.* **2002**, *82* (1 Pt 1), 50–63.

(13) Ratliff, F.; Hartline, H. K.; Miller, W. H. *J. Opt. Soc. Am.* **1963**, *53*, 110–20.

(14) He, Q.; Liu, Y. *Genes Dev.* **2005**, *19* (23), 2888–99.

(15) Asthagiri, A. R.; Nelson, C. M.; Horwitz, A. F.; Lauffenburger, D. A. *J. Biol. Chem.* **1999**, *274* (38), 27119–27.

(16) Hao, N.; Behar, M.; Elston, T. C.; Dohlman, H. G. *Oncogene* **2007**, *26* (22), 3254–66.

(17) Mettetal, J. T.; Muzzey, D.; Gómez-Uribe, C.; van Oudenaarden, A. *Science* **2008**, *319*, 482–4.

(18) Segel, L. A.; Goldbeter, A.; Devreotes, P. N.; Knox, B. E. *J. Theor. Biol.* **1986**, *120* (2), 151–79.

(19) Hauri, D. C.; Ross, J. *Biophys. J.* **1995**, *68*, 708–722.

(20) Spiro, P. A.; Parkinson, J. S.; Othmer, H. G. *Proc. Natl. Acad. Sci. U.S.A.* **1997**, *94* (14), 7263–8.

(21) Mello, B. A.; Tu, Y. *Proc. Natl. Acad. Sci. U.S.A.* **2005**, *102* (48), 17354–9.

(22) Barkai, N.; Leibler, S. *Nature* **1997**, *387* (6636), 913–7.

(23) Yi, T. M.; Huang, Y.; Simon, M. I.; Doyle, J. *Proc. Natl. Acad. Sci. U.S.A.* **2000**, *97* (9), 4649–53.

(24) Csikasz-Nagy, A.; Soyer, O. S. *J. R. Soc. Interface* **2008**, *5*, S41–S47.

(25) Wilkie, J.; Johnson, M.; Reza, K. *Control Engineering. An Introductory Course*; Palgrave: New York, 2002.

(26) Milsum, J. H. *Biological Control Systems Analysis*; McGraw-Hill: New York, 1966.

(27) Ingalls, B. P.; Yi, T.-M.; Iglesias, P. A. In *System Modeling in Cellular Biology*; Szallasi, Z., Stelling, J., Periwal, V., Eds.; MIT Press: Cambridge, MA, 2006.

(28) El-Samad, H.; Goff, J. P.; Khammash, M. *J. Theor. Biol.* **2002**, *214* (1), 17–29.

(29) Sontag, E. D. *Mathematical Control Theory. Deterministic Finite Dimensional Systems*, 2nd ed.; Springer-Verlag: New York, 1998.

(30) Ruoff, P.; Loros, J. J.; Dunlap, J. C. *Proc. Natl. Acad. Sci. U.S.A.* **2005**, *102* (49), 17681–6.

(31) Ruoff, P.; Zakhartsev, M.; Westerhoff, H. V. *FEBS J.* **2007**, *274* (4), 940–50.

(32) Savageau, M. A. *Nature* **1971**, *229* (5286), 542–4.

(33) Savageau, M. A. *Biochemical Systems Analysis. A Study of Function and Design in Molecular Biology*; Addison-Wesley: Reading, MA, 1976.

(34) Fell, D. *Understanding the Control of Metabolism*; Portland Press: London and Miami, FL, 1997.

(35) Heinrich, R.; Schuster, S. *The Regulation of Cellular Systems*; Chapman and Hall: New York, 1996.

(36) Ruoff, P. Perfect Adaptation with Zero Control Coefficients, KITP. http://online.itp.ucsb.edu/online/bioclocks07/ruoff1/.

(37) Radhakrishnan, K.; Hindmarsh, A. C. *Description and Use of LSODE, the Livermore Solver for Ordinary Differential Equations*. NASA Reference Publication 1327, Lawrence Livermore National Laboratory Report UCRL-ID-113855; National Aeronautics and Space Administration, Lewis Research Center: Cleveland, OH, 1993.

(38) Burns, J. A.; Cornish-Bowden, A.; Groen, A. K.; Heinrich, R.; Kacser, H.; Porteous, J. W.; Rapoport, S. M.; Rapoport, T. A.; Stucki, J. W.; Tager, J. M.; Wanders, R. J. A.; Westerhoff, H. V. *Trends Biochem. Sci.* **1985**, *19*, 16.

(39) Ingalls, B. P. *J. Phys. Chem. B* **2004**, *108*, 1143–1152.

(40) Brodie, S. E.; Knight, B. W.; Ratliff, F. *J. Gen. Physiol.* **1978**, *72* (2), 167–202.

(41) Alon, U. *An Introduction to Systems Biology: Design Principles of Biological Circuits*; Chapman & Hall: New York, 2006.

(42) Kondepudi, D.; Prigogine, I. *Modern Thermodynamics. From Heat Engines to Dissipative Structures*; John Wiley & Sons: Chichester, U.K., 1998.

(43) von Bertalanffy, L. *Perspectives on General System Theory*; George Braziller: New York, 1975.

(44) Moore, J. W.; Pearson, R. G. *Kinetics and Mechanism*, 3rd ed.; John Wiley & Sons: New York, 1981.

(45) Wagner, A. *Robustness and Evolvability in Living Systems*; Princeton University Press: Princeton, NJ, 2005.

(46) Kitano, H. *Mol. Syst. Biol.* **2007**, *3*, 1–7.

(47) Hastings, J. W.; Sweeney, B. M. *Proc. Natl. Acad. Sci. U.S.A.* **1957**, *43*, 804–811.

(48) Hazel, J. R.; Prosser, C. L. *Physiol. Rev.* **1974**, *54* (3), 620–677.

(49) Ruoff, P. *J. Interdiscip. Cycle Res.* **1992**, *23*, 92–99.

(50) Edwards, K. D.; Lynn, J. R.; Gyula, P.; Nagy, F.; Millar, A. J. *Genetics* **2005**, *170* (1), 387–400.

(51) Eckhardt, N. A. *Plant Cell* **2006**, *18* (5), 1105–08.

(52) Gould, P. D.; Locke, J. C.; Larue, C.; Southern, M.; Davis, S. J.; Hanano, S.; Moyle, R.; Milich, R.; Putterill, J.; Millar, A. J.; Hall, A. *Plant Cell* **2006**, *18* (5), 1177–87.

(53) Kholodenko, B. N.; Kiyatkin, A.; Bruggeman, F. J.; Sontag, E.; Westerhoff, H. V.; Hoek, J. B. *Proc. Natl. Acad. Sci. U.S.A.* **2002**, *99* (20), 12841–6.

(54) Ross, J. *J. Phys. Chem. A* **2008**, *112* (11), 2134–43.

(55) Ruoff, P.; Noyes, R. J. *J. Phys. Chem.* **1985**, *89*, 1339–1341.

(56) Ermentrout, B. *Simulating, Analyzing, and Animating Dynamical Systems. A Guide to XPPAUT for Researchers and Students*; Society for Industrial and Applied Mathematics: Philadelphia, PA, 2002.

(57) Szallasi, Z.; Stelling, J.; Periwal, V. *System Modeling in Cellular Biology*; MIT Press: Cambridge, MA, 2006.

JP806818C